SAND2011-4466C

Simulations of Dynamic Laser / Plasma X-ray Production*

D. R. Welch, C. L. Miller, D. V. Rose
Voss Scientific, LLC
R. B. Campbell, B. V. Oliver, T. J. Webb, D. G. Flicker
Sandia National Laboratories

18th IEEE International Pulsed Power Conference
21 June 2011

* Work supported by Sandia National Laboratories. Sandia National Laboratories is a multi-program laboratory operated by Sandia Corporation, a wholly owned subsidiary of Lockheed Martin Company, for the United States Department of Energy's National Nuclear Security Administration under contract DE-AC04-94-AL85000.

Basic Simulation Parameters

The picosecond-scale, IR laser pulse strikes a dense thin-foil gold target, where the high field intensity accelerates electrons to high energies. These electrons propagate through the dense gold plasma, where the electron-ion interaction produces bremsstrahlung X-rays, which are then transported to the edges of the simulation space. Once an X-ray macroparticle reaches the edge of the simulation space, ensuring its interaction with the target was over, the x-, y-, and z-components of its momentum and location, along with the time and macroparticle weight are saved to a particle extraction file. These particle extraction files, one for each boundary face, can be used as inputs for a simple transport simulation that carry the particles to a spherical target with a 1 meter radius. Here, the X-ray number fluences are scaled by a factor of 2.6×10^{-10} (characteristic of a several-MV diode source) to get a reasonable estimate of the dose -- a strictly accurate dose calculation would depend on the detailed energy spectrum of the X-rays and the specific detector.

- Peak Au^{2+} density of 6e22 cm^{-3}
- Foil thickness of 10 μm, 20 μm blow-off plasma, 50 μm foil radius, 30º foil angle
- Gaussian laser spot of 10 μm; 80 J laser in 1.4 ps, $5x10^{19}$ W/cm^2
- Scale number fluence by 2.6e-10 to get dose
- Also scale from measurement location to 1-meter radius

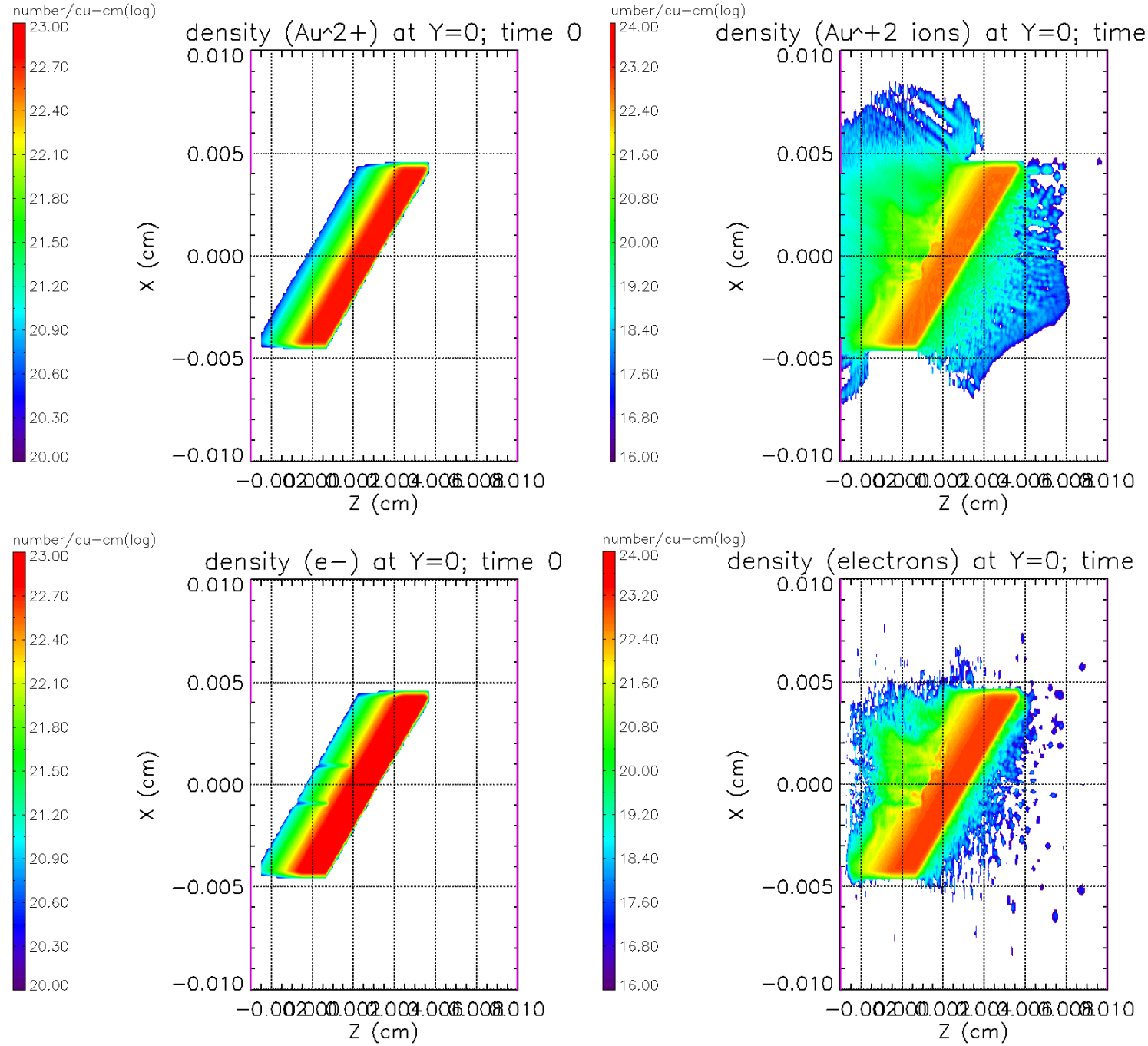

Figure 18. Cross-section plot from the P-polarized simulation at y = 0 and t = 10 ps of number density for: doubly ionized gold ions (left) and electrons (right).

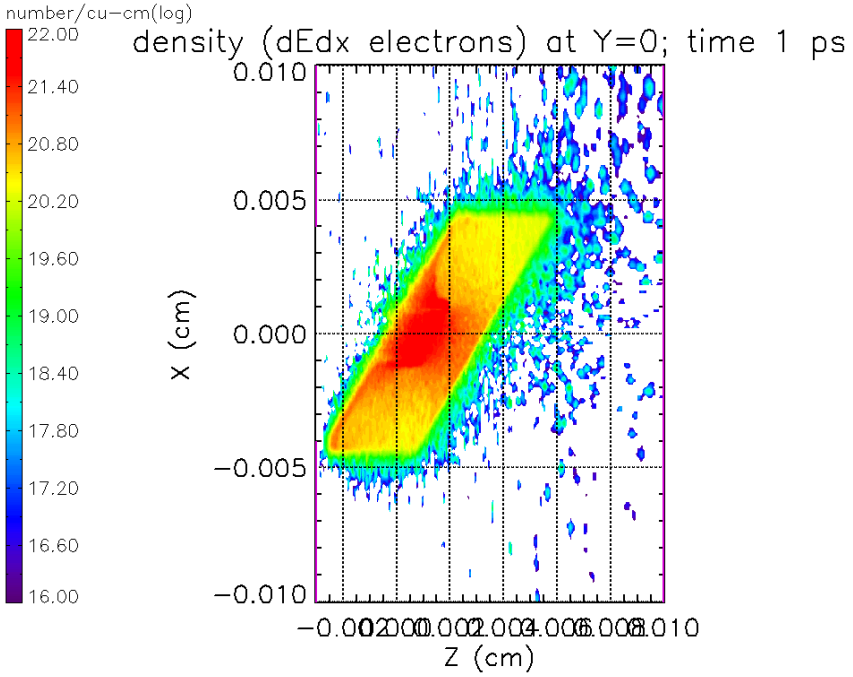
number/cu-cm(log)
22.00
21.40
20.80
20.20
19.60
19.00
18.40
17.80
17.20
16.60
16.00
density (dEdx electrons) at Y=0; time 1 ps
0.010
0.005
0.000
−0.005
−0.010
X (cm)
Z (cm)

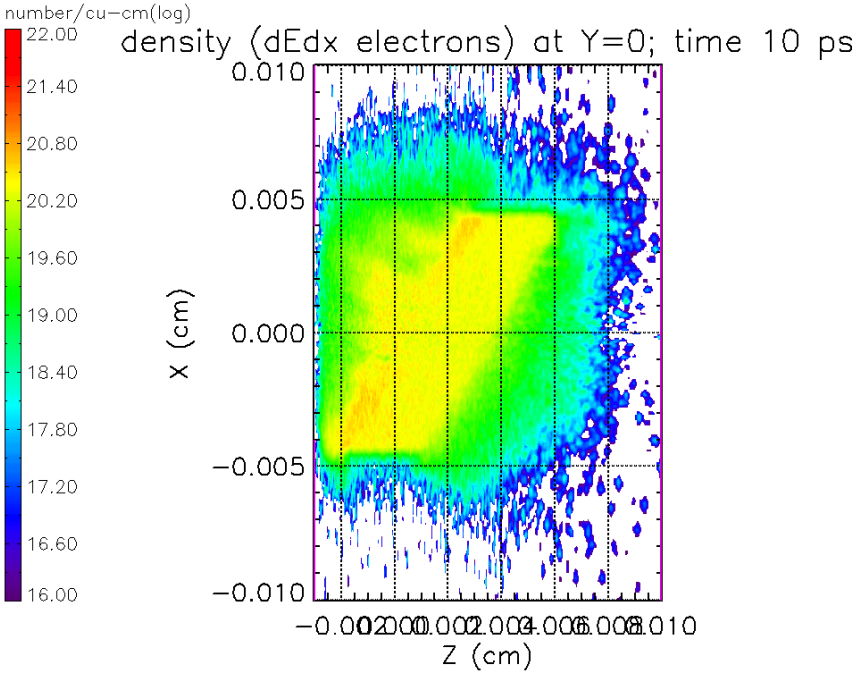
number/cu-cm(log)
22.00
21.40
20.80
20.20
19.60
19.00
18.40
17.80
17.20
16.60
16.00
density (dEdx electrons) at Y=0; time 10 ps
0.010
0.005
0.000
−0.005
−0.010
X (cm)
Z (cm)

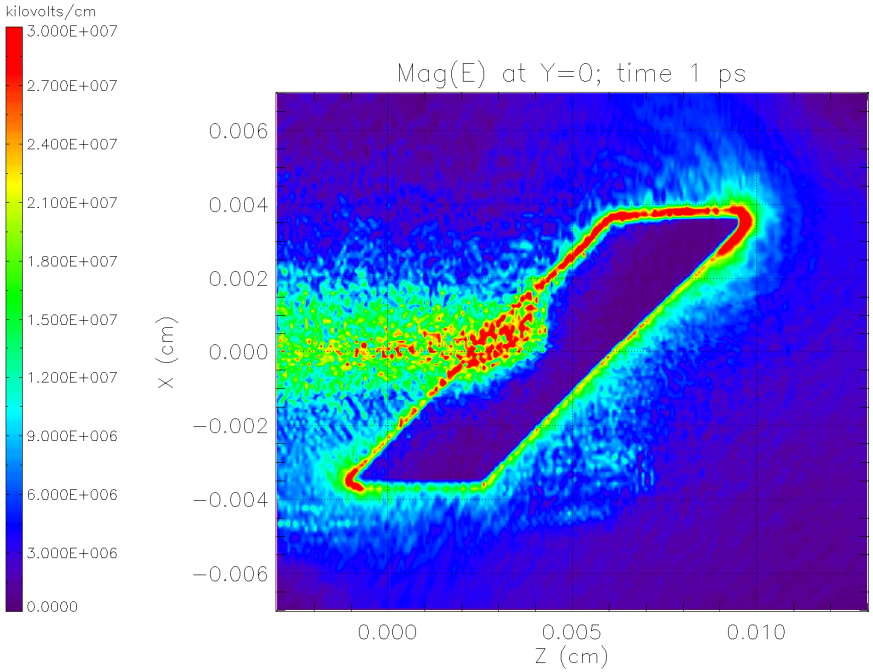
kilovolts/cm
3.000E+007
2.700E+007
2.400E+007
2.100E+007
1.800E+007
1.500E+007
1.200E+007
9.000E+006
6.000E+006
3.000E+006
0.0000
Mag(E) at Y=0; time 1 ps
0.006
0.004
0.002
0.000
−0.002
−0.004
−0.006
X (cm)
0.000
0.005
0.010
Z (cm)

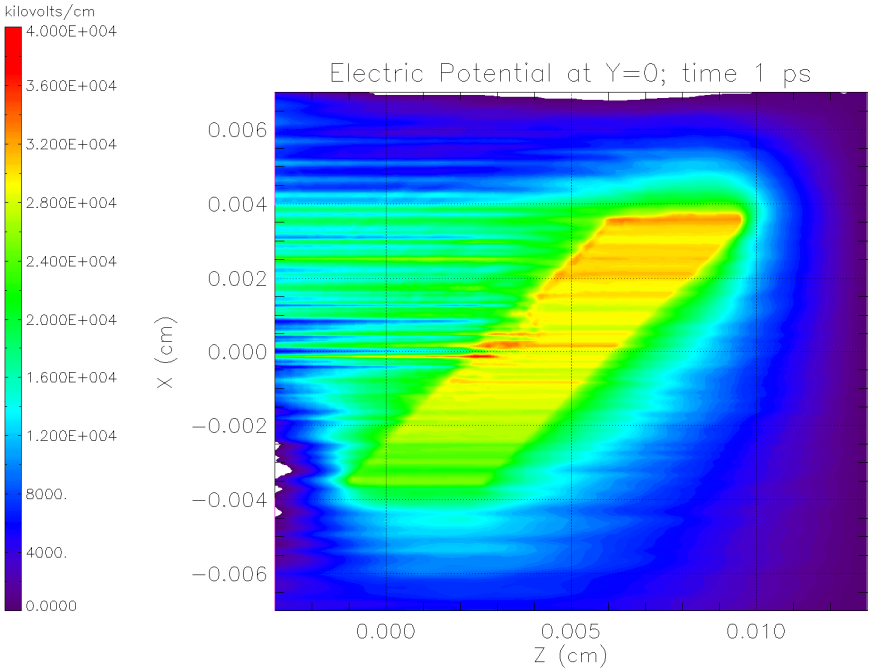
kilovolts/cm
4.000E+004
3.600E+004
3.200E+004
2.800E+004
2.400E+004
2.000E+004
1.600E+004
1.200E+004
8000.
4000.
0.0000
Electric Potential at Y=0; time 1 ps
0.006
0.004
0.002
0.000
−0.002
−0.004
−0.006
X (cm)
0.000
0.005
0.010
Z (cm)

10 μm thick, 50 μm radius, 30º tilt Au foil – 2D

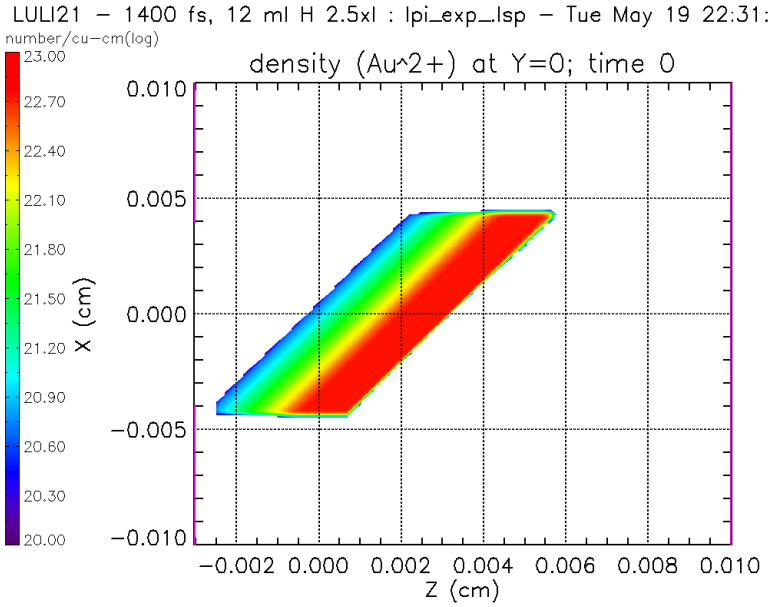

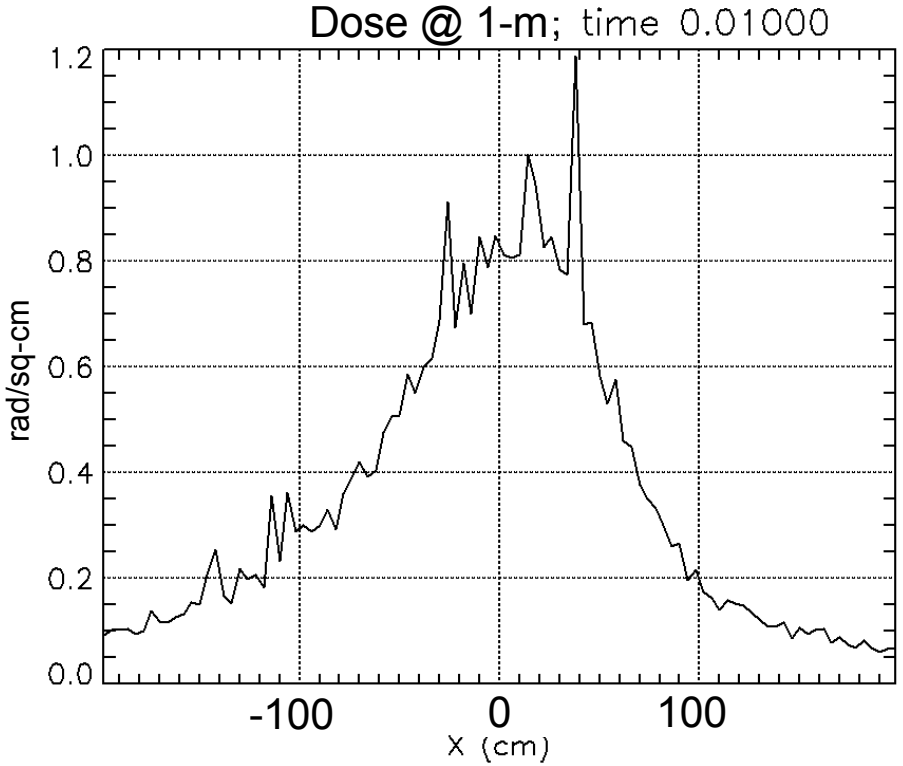

- 2D Cartesian simulation to 10 ps
- 1 cm effective virtual dimension width
- Dose averaged @ 1-m is 358.8 mRad (1.38e9 cm^{-2})

Tilt Angle	Peak Fluence (cm^{-3})	Average Fluence (cm^{-3})	Average Dose (mRad)
0º	2.04×10^{9}	1.06×10^{9}	275.6
10º	3.28×10^{9}	1.32×10^{9}	343.2
20º	2.76×10^{9}	1.13×10^{9}	293.8
30º	4.57×10^{9}	1.38×10^{9}	358.8

Fully 3D Simulations

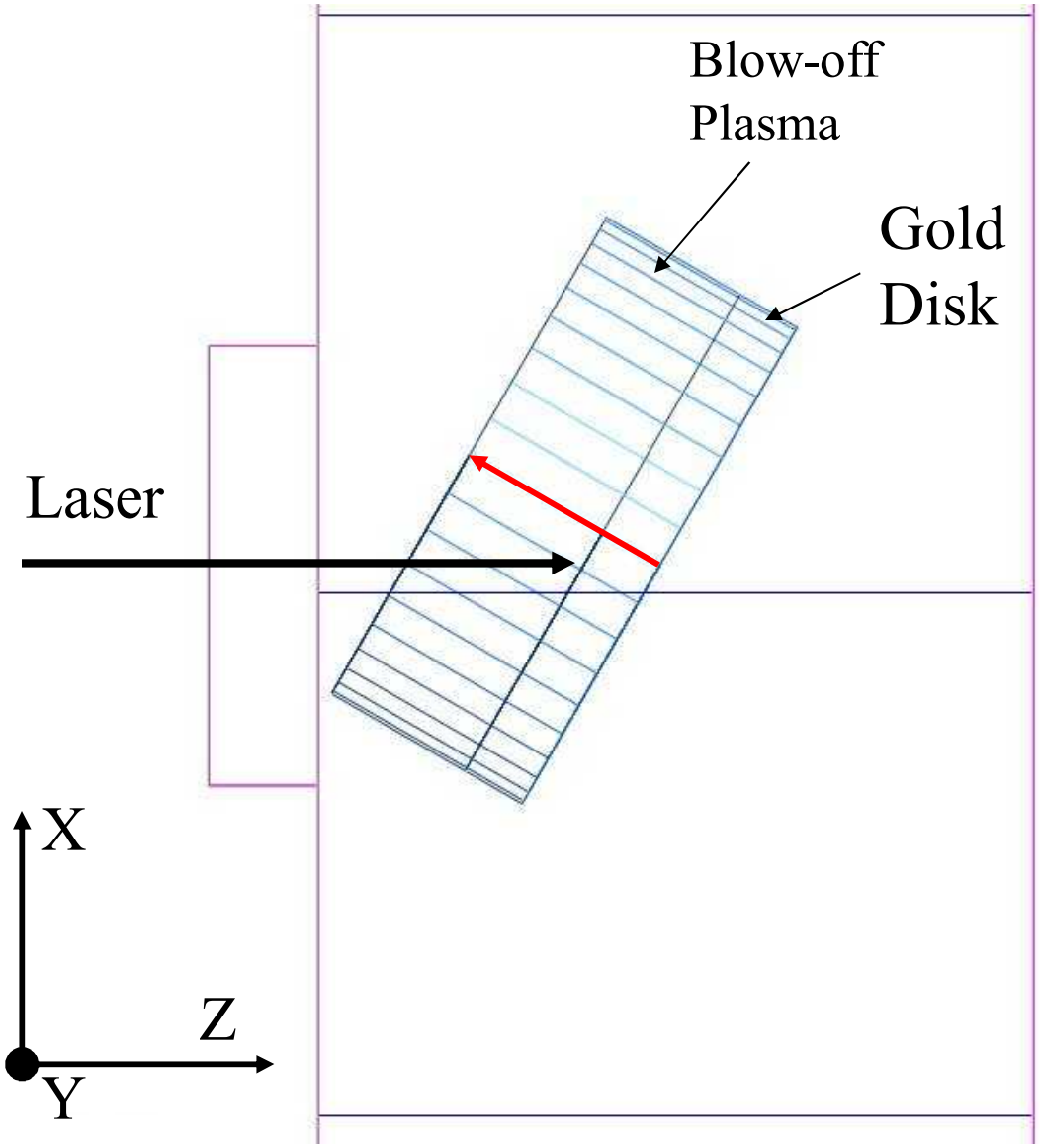

- Laser incident along Z-axis in positive direction
- X-polarized E-field → P-pol
- Y-polarized E-field → S-pol

- Typical gold number density:

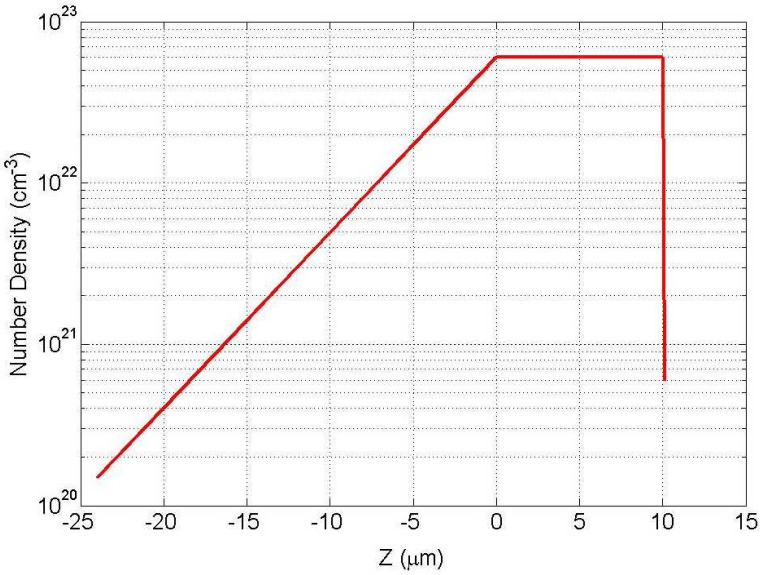

10 μm thick, variable radius, 0º tilt Au foil

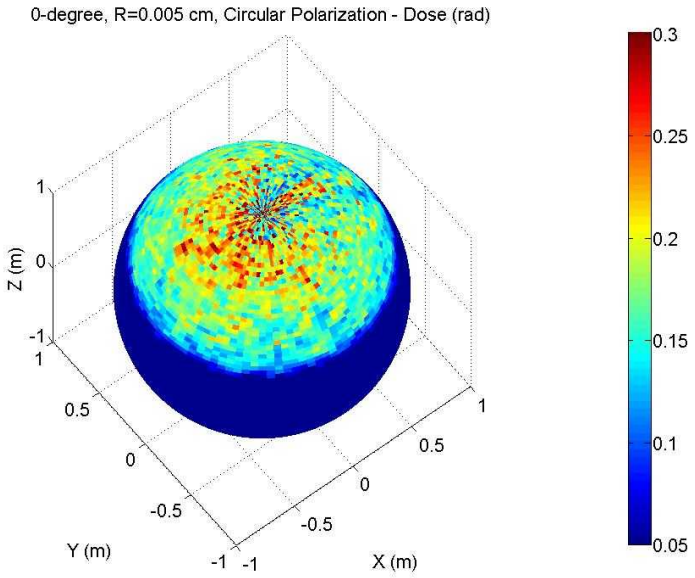

- 3D cylindrical simulation to 10 ps
- Dose @ 1-meter is:
  - 150-250 mRad for R=50 μm
  - 130-220 mRad for R=100 μm
  - 100-200 mRad for R=150 μm

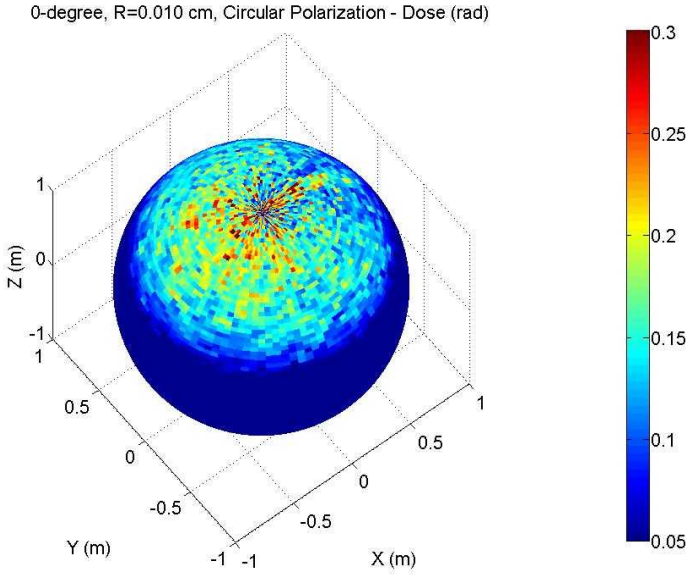

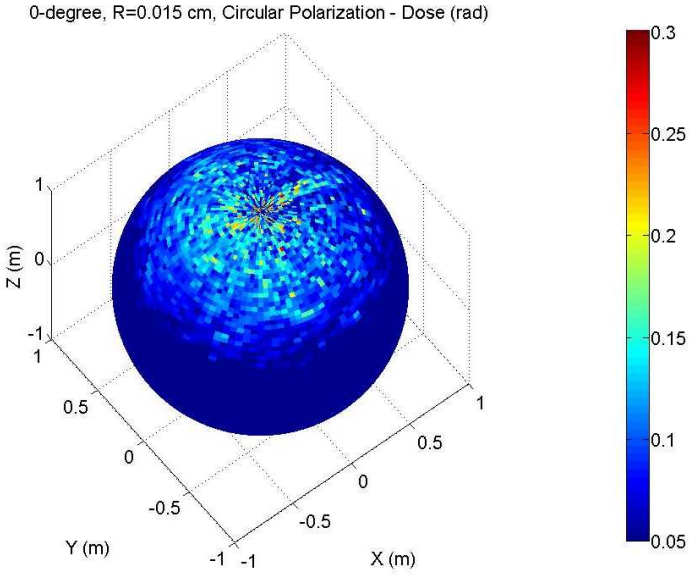

Simulation Space Decomposition

- Large number of particles in the simulation space (~3.85e8) means careful partitioning can improve simulation time
- Complicated by non-uniform gridding in all dimensions
- Volume broken into 8 regions
- First division, in X, divided particles evenly between top and bottom half

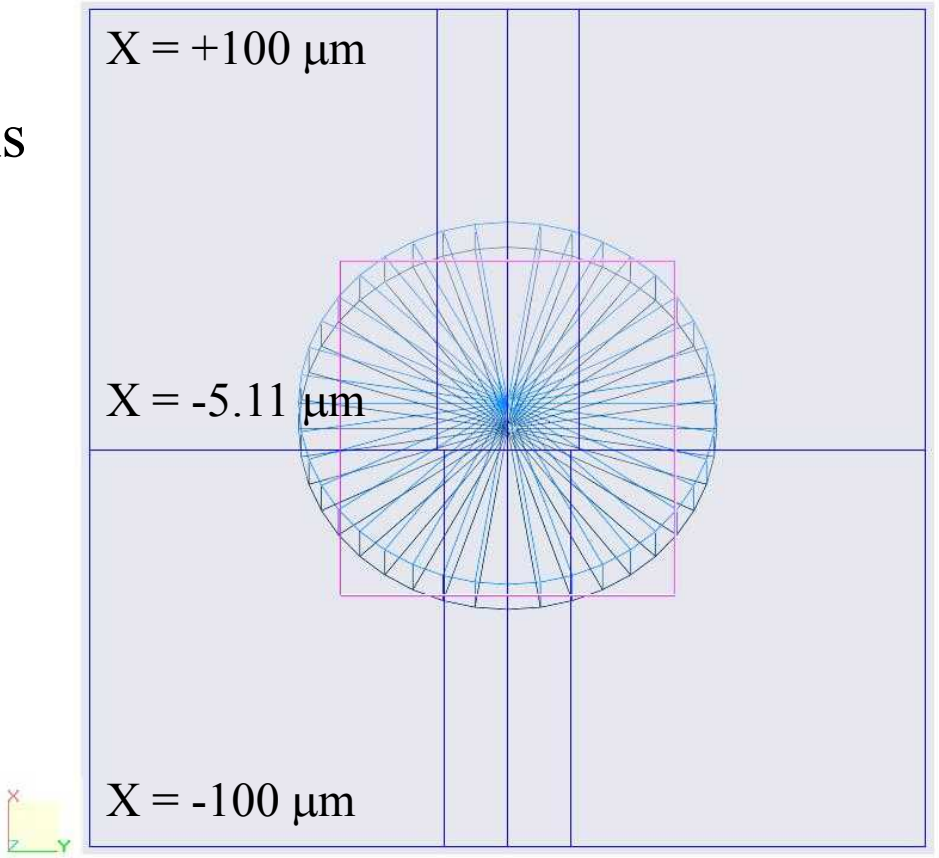

- Second division, in Y, divides particles evenly into each of the four regions – smaller Y-extent in the center reflects smaller gridding
- Final division, in Z, puts particles into 48 evenly-sized domains and adds 6 larger domains for field solve before and after disk

X-ray Histories – 3D Cartesian, P-Pol

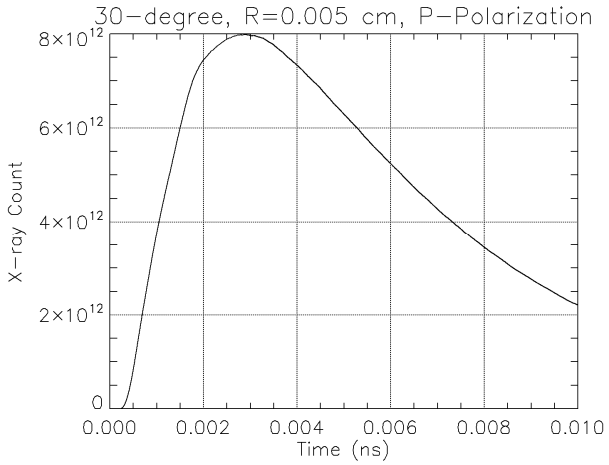

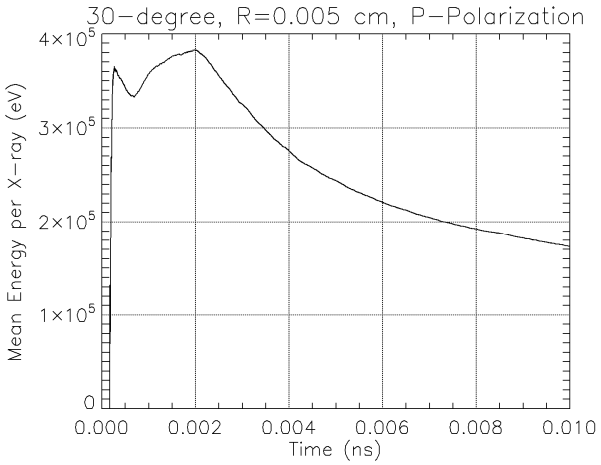

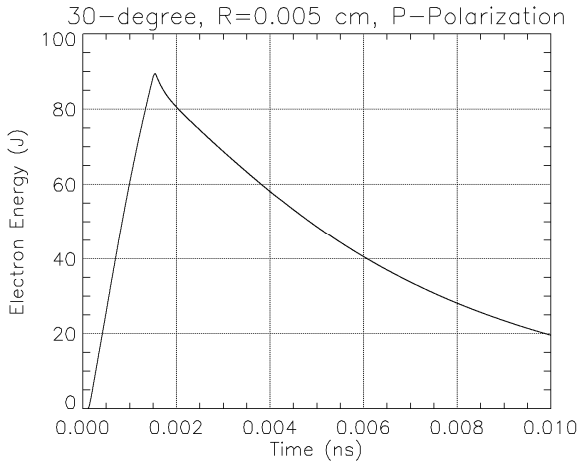

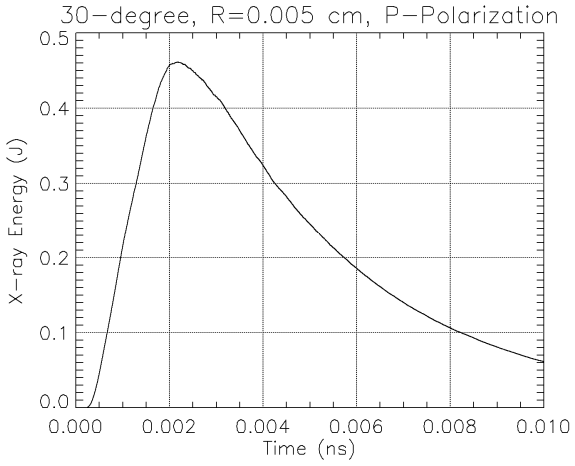

- 130 J total incident field energy
- Total x-ray production of 8.66e13
- Dose averaged over entire target @ 1-meter is 179.2 mRad (6.89e8 cm^{-2})
- Time histories of global X-ray count, total X-ray energy, and energy per X-ray for the 3D Cartesian P-Polarization simulation.

X-ray Histories – 3D Cartesian, S-Pol

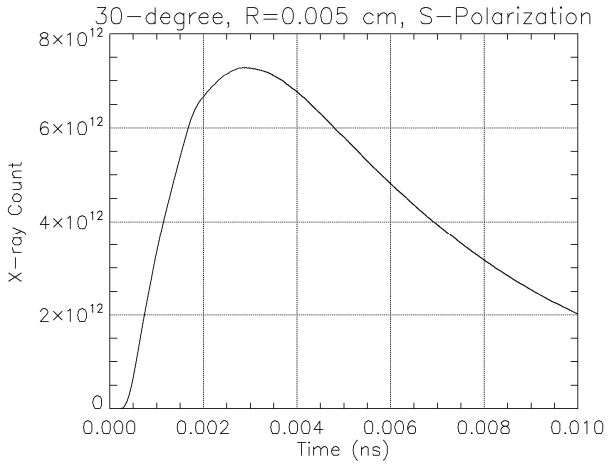

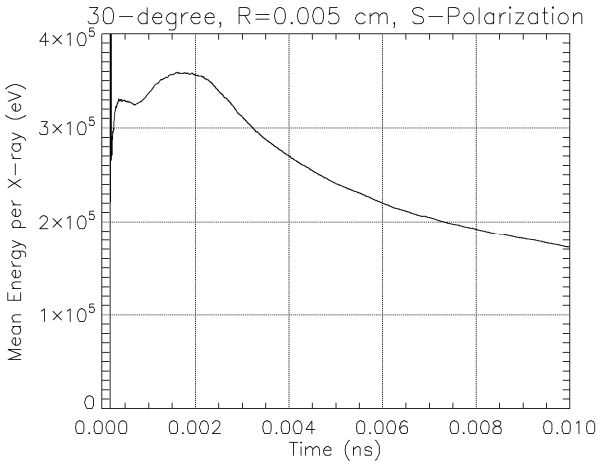

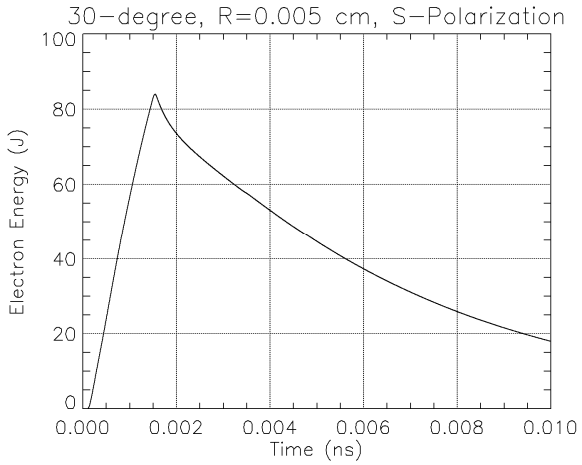

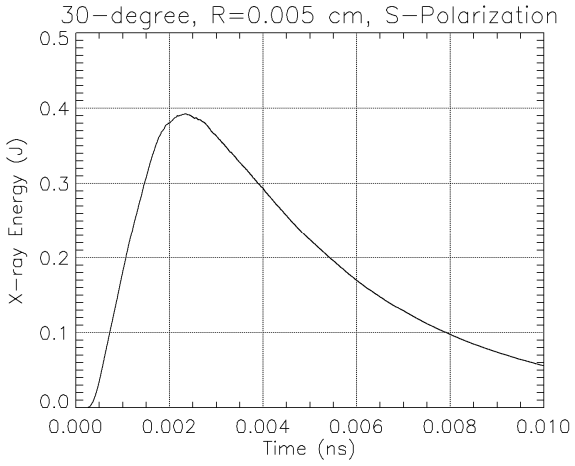

- 130 J total incident field energy
- Total x-ray production of 7.78e13
- Dose averaged over entire target @ 1-meter is 161.0 mRad (6.19e8 cm^{-2})
- Time histories of global X-ray count, total X-ray energy, and energy per X-ray for the 3D Cartesian S-Polarization simulation.

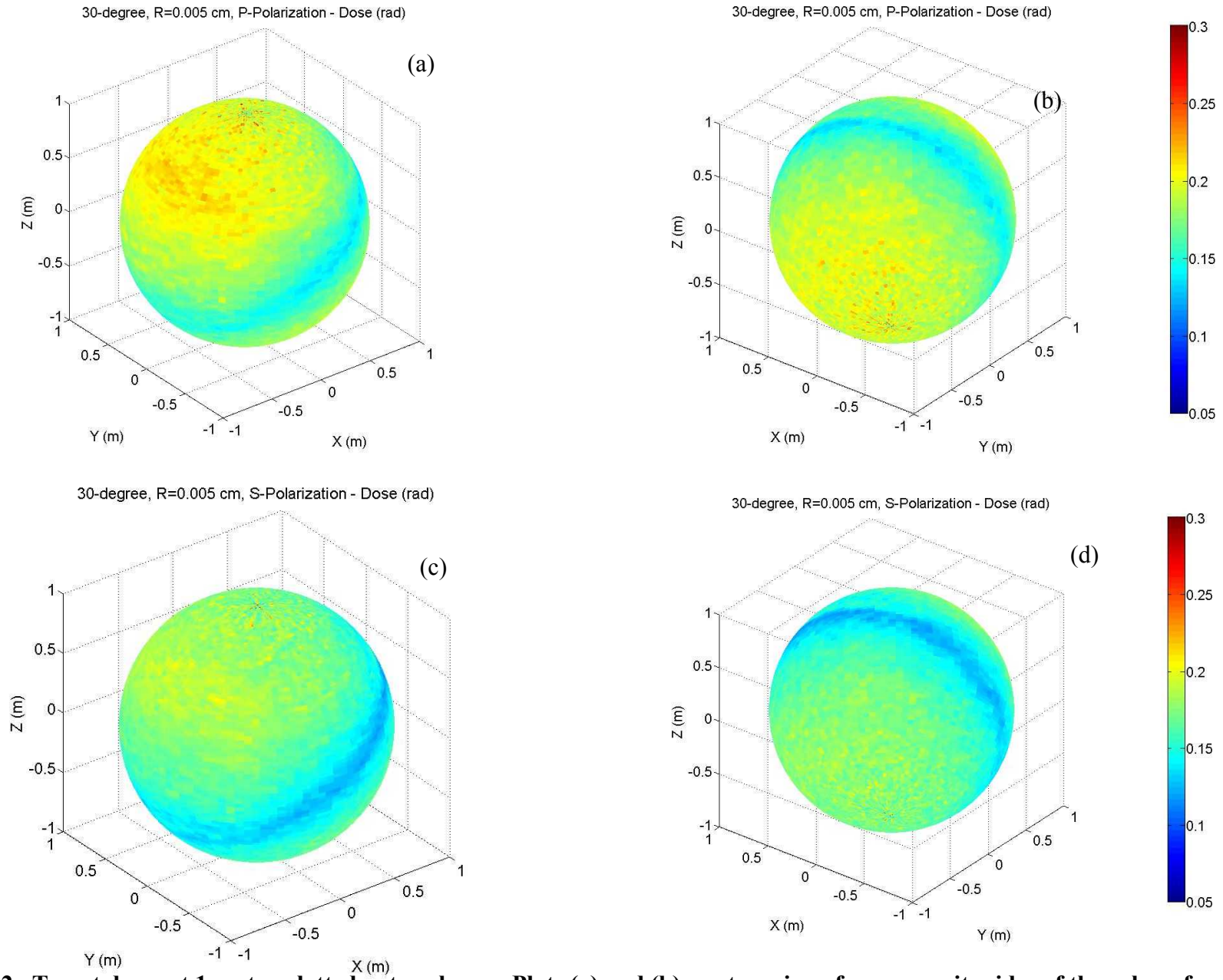

Figure 22. Target doses at 1-meter plotted onto spheres. Plots (a) and (b) are two views from opposite sides of the sphere for the P-Polarization case; (c) and (d) are the same views for the S-Polarization.

SNL Fielded Geometry

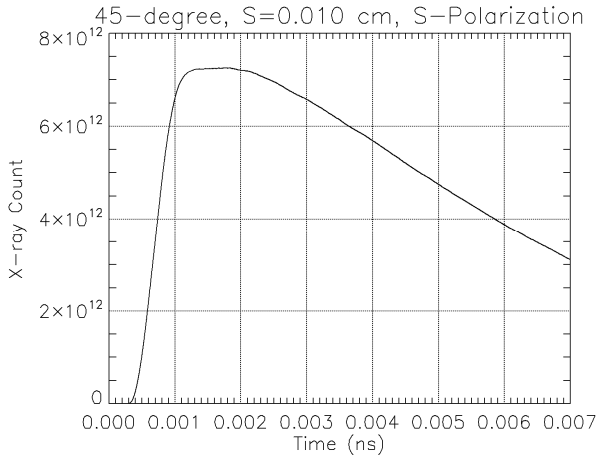

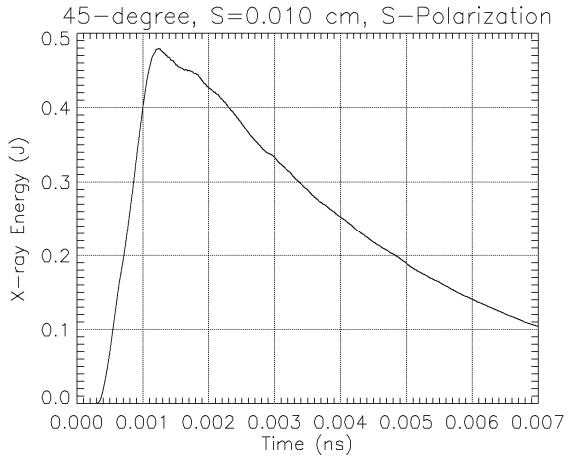

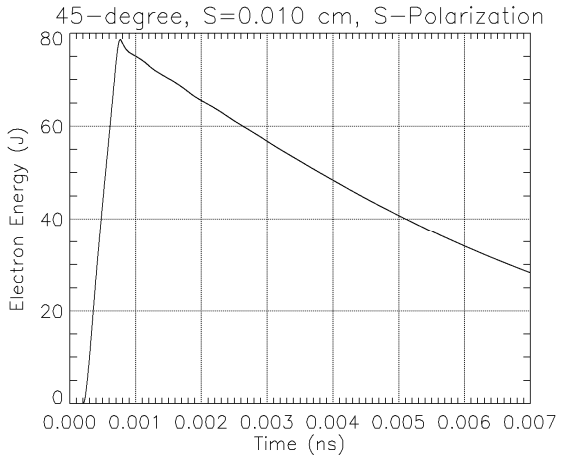

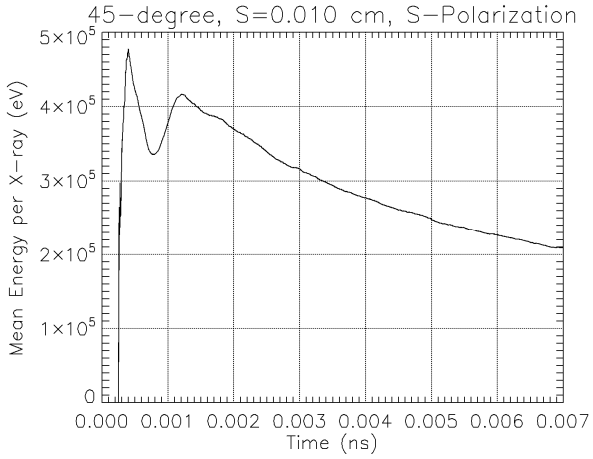

- New geometry requested to match SNL experiments
- Square foil with S = 100 μm, 45-degree tilt
- 500 fs duration, a 5.9 μm FWHM spot size, and a total incident field energy of ~100 J
- Simulation only ran to 7 ps – results scaled up by 20% to compare to 10 ps runs
- 8.60×10^{13} total X-rays and 178.0 mRad, averaged at 1-meter

The scaled 1 meter dose shows values from 220 mRad (near the disk axes) to 140 mRad (near the disk edge). This lower value matches with experimentally measured values on the foil edge that were on the order of 100 mRad.

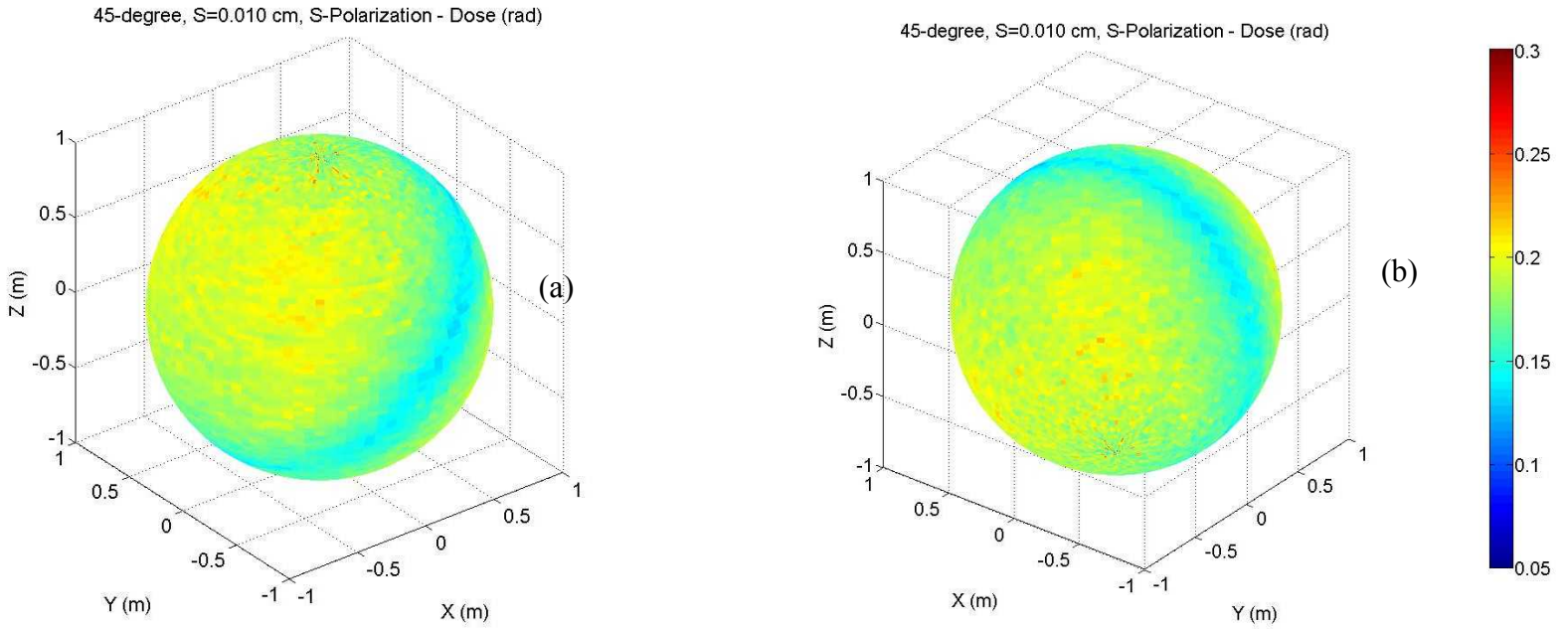

Target doses at 1-meter plotted onto spheres. Plots (a) and (b) have the fluences scaled up by 20% to estimate the dose at 10 ps.

Global X-ray Spectra – 3D Cartesian

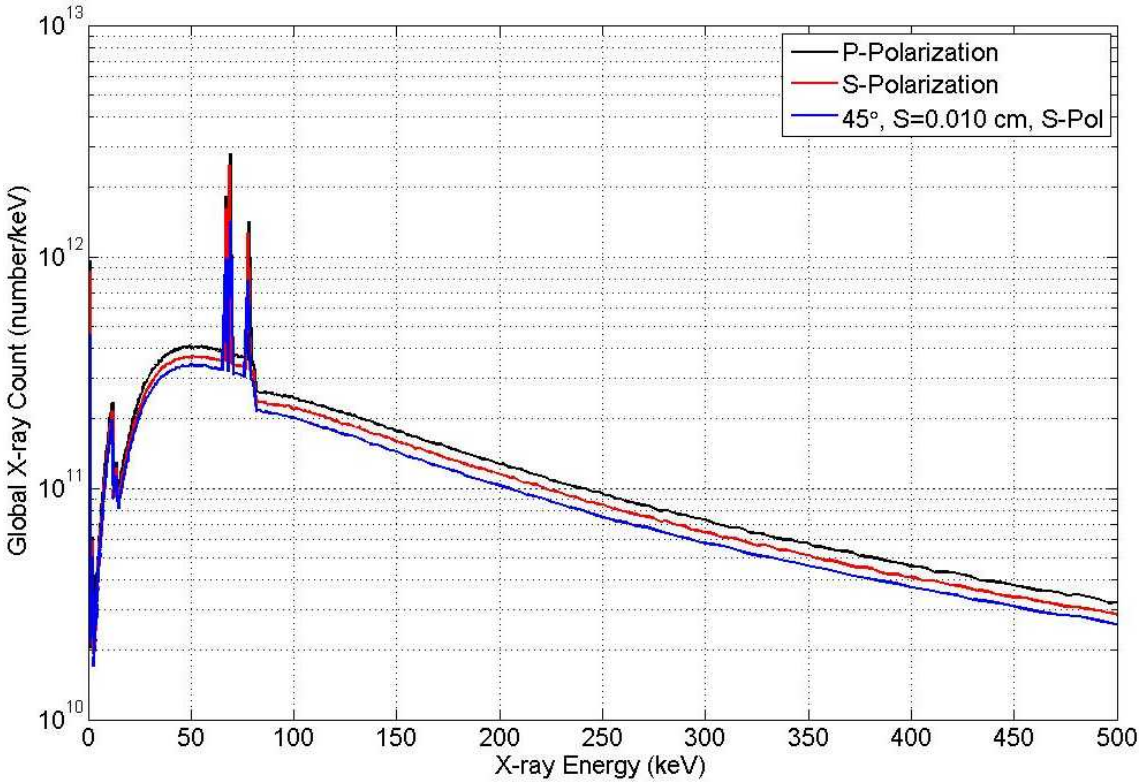

Global X-ray spectra for the two polarizations and SNL geometry. The differences arise from the different X-ray counts for the three cases.

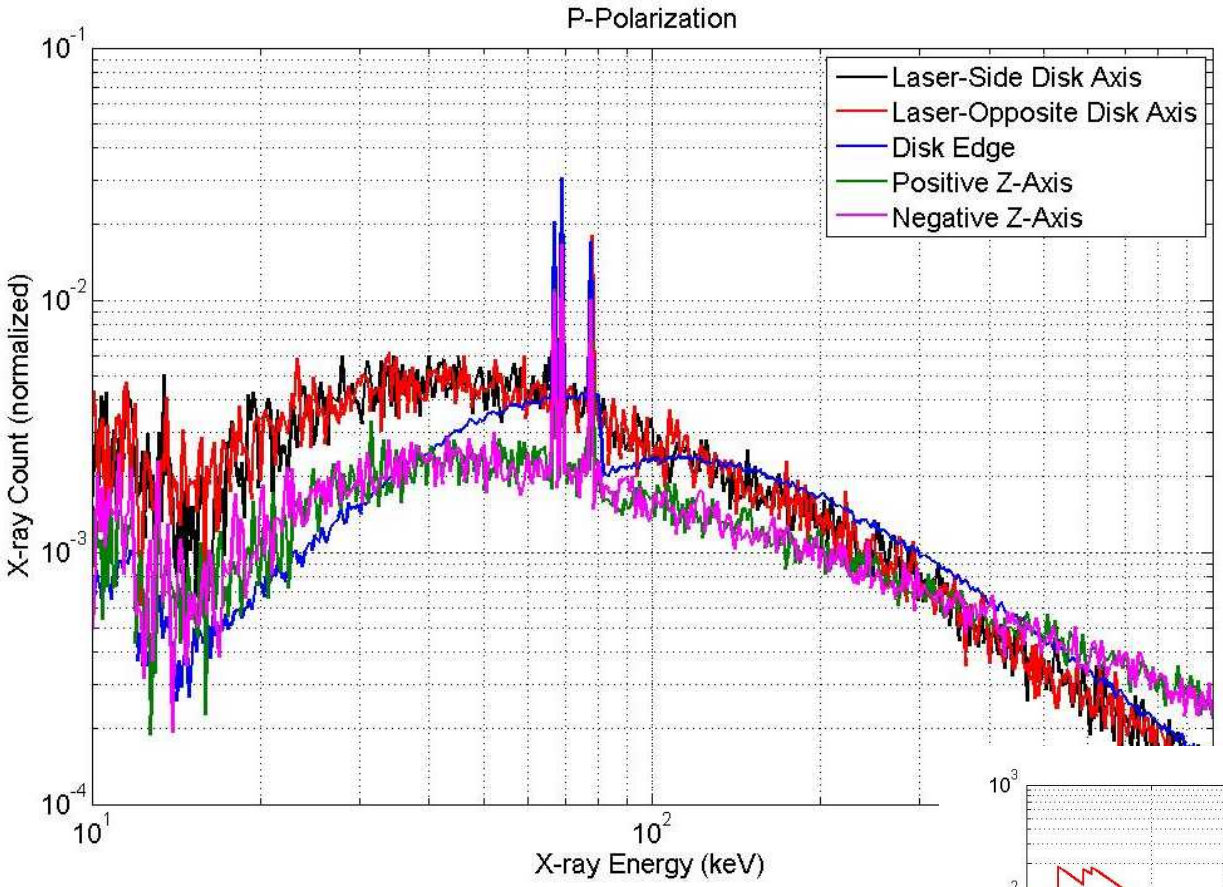

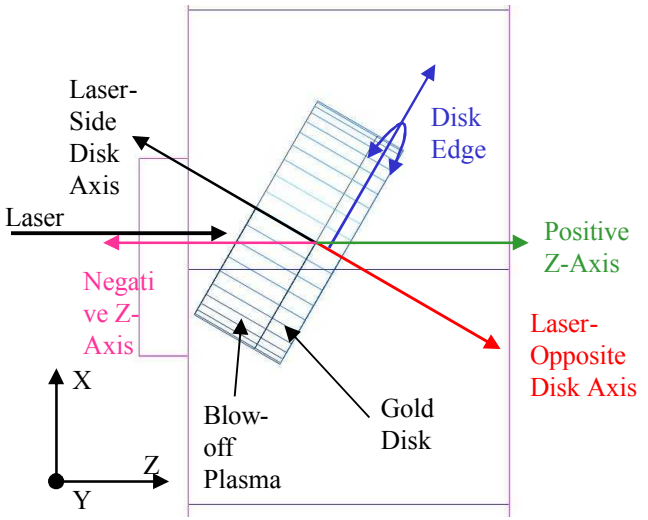

- Spectra normalized to integrate to 1
- Disk edge shows a harder spectrum due to preferential absorption of lower-energy X-rays by the disk

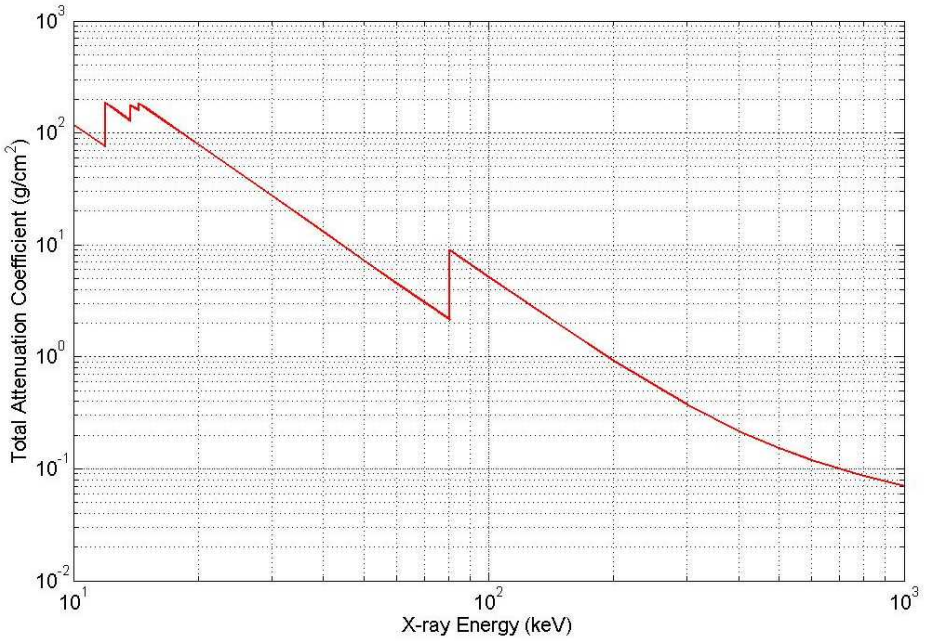

Conclusions

- LSP used to model full physics of a dynamic laser / plasma interaction and bremsstrahlung X-ray production
- X-ray production is very sensitive to foil size, but fairly insensitive to incident laser angle
- Typical 1-meter dose for targets of interest is in the 100-200 mRad range, but shows significant angular variation
- This dose matches experimental values
- Energy spectra also show strong variations with angle due to self-absorption by the foil – this has consequences for the accurate dose calculation
- Future work could explore the effect of alignment jitter or blow-off characteristic length

References

1. R. B. Campbell and B. V. Oliver, LDRD proposal (2009).
2. P. Rambo, J. Schwarz, M. Geissel, E. Brambrink, A. Edens, M. Kimmel, and B. Atherton, "The Z-Petawatt Laser at Sandia National Laboratories," in Conference on Lasers and Electro-Optics/Quantum Electronics and Laser Science Conference and Photonic Applications Systems Technologies, OSA Technical Digest (CD), paper JTuA50 (2008).
3. L. E. Ruggles, J. L. Porter, P. K. Rambo, W. W. Simpson, M. F. Vargas, G. R. Bennett, and I. C. Smith, "Measurements of 4–10 keV x-ray production with the Z-Beamlet laser," Rev. Sci. Instrum. 74, 2206 (2003).
4. G. R. Bennett, O. L. Landen, R. F. Adams, J. L. Porter, L. E. Ruggles, W. W. Simpson, and C. Wakefield, "X-ray imaging techniques on Z using the Z-Beamlet laser," Rev. Sci. Instrum. 72, 657 (2001).
5. R. D. Edwards, M. A. Sinclair, T. J. Goldsack, et al., "Characterization of a gamma-ray source based on a laser-plasma accelerator with applications to radiography," Appl. Phys. Lett. 80, 2129 (2002).
6. J. Galy, M. Maučec, D. J. Hamilton, R. Edwards, and J. Magill, "Bremsstrahlung production with high-intensity laser matter interactions and applications," New J. Phys. 9, 23 (2007).
7. D. R. Welch, D. V. Rose, M. E. Cuneo, R. B. Campbell, and T. A. Mehlorn, "Integrated simulation of the generation and transport of proton beams from laser-target interaction," Phys. Plasmas 13, 063105 (2006).
8. C. Thoma, R. E. Clark, T. C. Genoni, and B. V. Oliver, "Lsp simulations of laser plasma interactions for applications to laser-driven radiography," Mission Research Report No. MRC/ABQ-R-2092 (2003).
9. D. R. Welch D. R. Welch, D.V. Rose, R. E. Clark, C. B. Mostrom, W. A. Stygar, and R. J. Leeper, "Fully kinetic particle-in-cell simulations of a deuterium gas puff z pinch," Phys. Rev. Lett. 103, 255002 (2009).
10. S. Balay, W. D. Gropp, L. C. McInnes, and B. F. Smith, "Efficient Management of Parallelism in Object Oriented Numerical Software Libraries," in Modern Software Tools in Scientific Computing, edited by E. Arge, A. M. Bruaset, and H. P. Langtangen, pp. 163-202. Birkhäuser Press (1997).
11. J. A. Halbleib, R. P. Kensek, G. D. Valdez, S. M. Seltzer, and M. J. Berger, "ITS: The Integrated TIGER Series of electron/photon transport codes - version 3.0," IEEE Trans. Nucl. Sci. NS-39, 1025 (1992).
12. D. V. Rose, D. R. Welch, et al., "Coupled particle-in-cell and Monte Carlo transport modeling of intense radiographic sources," J. Appl. Phys. 91, 3328 (2002).
13. D. R. Welch, C. L. Miller, R. B. Campbell, and B. V. Oliver, "Laser radiography," Voss Scientific Report VSL-0914 (2009).
14. M. J. Berger, J. H. Hubbell, S. M. Seltzer, J. Chang, J. S. Coursey, R. Sukumar, and D. S. Zucker, "XCOM: Photon Cross Sections Database," http://www.nist.gov/physlab/data/xcom/index.cfm (retrieved 22 September 2010).

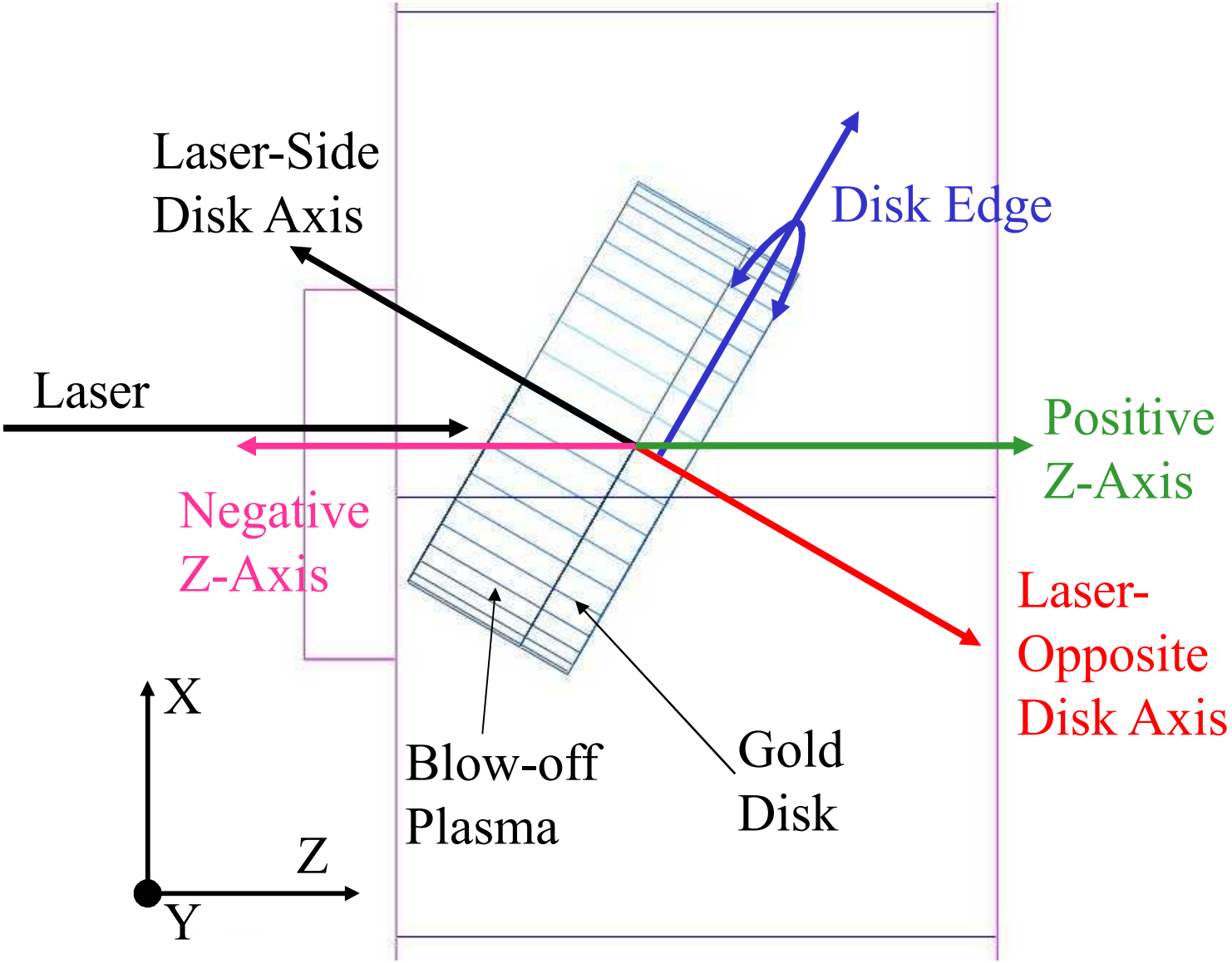
Laser-Side
Disk Axis
Disk Edge
Laser
Positive
Z-Axis
Negative
Z-Axis
Laser-
Opposite
Disk Axis
X
Z
Y
Blow-off
Plasma
Gold
Disk